Published in final edited form as:
Cancer Res. 2008 August 1; 68(15): 6396–6406. doi:10.1158/0008-5472.CAN-08-0645.

Targeted Overexpression of Vav3 Oncogene in Prostatic Epithelium Induces Nonbacterial Prostatitis and Prostate Cancer

Yin Liu[1], **Jun Qin Mo**[1], **Qiande Hu**[2], **Gregory Boivin**[1], **Linda Levin**[3], **Shan Lu**[2], **Dianer Yang**[2], **Zhongyun Dong**[2], and **Shan Lu**[1]

[1] Department of Pathology, University of Cincinnati College of Medicine, Cincinnati, Ohio

[2] Department of Medicine, University of Cincinnati College of Medicine, Cincinnati, Ohio

[3] Department of Environmental Heath, University of Cincinnati College of Medicine, Cincinnati, Ohio

Abstract

Our previous study revealed that Vav3 oncogene is overexpressed in human prostate cancer, activates androgen receptor (AR), and stimulates growth in prostate cancer cells. The purpose of this study is to further determine the potential role of Vav3 in prostate cancer development in genetically engineered mouse model. We generated Vav3 transgenic mice by targeted overexpression of a constitutive active Vav3 in the prostatic epithelium. We found that overexpression of Vav3 led to development of mouse prostatic intraepithelial neoplasia and prostate cancer at the age of as early as 3 months. The AR signaling axis and phosphatidylinositol 3-kinase-Akt signaling were elevated in the prostate glands of Vav3 transgenic mice. In addition to prostate cancer, Vav3 transgenic mice developed significant nonbacterial chronic prostatitis in the prostate gland with notable infiltration of lymphomononuclear cells (monocytes, lymphocytes, and plasma cells), which was associated with elevated incidence of prostate cancer. DNA microarray and signaling pathway analysis revealed that the top diseases and disorders were inflammatory diseases and cancer of the prostate gland in Vav3 transgenic mice. *In vitro* analysis showed that overexpression of Vav3 in prostate cancer cells enhanced nuclear factor-κB (NF-κB) activity, implicating an underlying mechanism of innate inflammatory response induced by elevated Vav3 activity. These data showed that Vav3 overexpression in the prostate epithelium enhanced both the AR signaling axis and NF-κB–mediated pathway, which potentially contributed to the development of nonbacterial prostatitis and prostate cancer.

Introduction

It was widely accepted that inflammation contributes to cancer development (1,2). Many cancers, such as hepatocellular carcinoma, stomach cancer, and colorectal carcinoma, arise from chronic infection and inflammation. Compelling data indicate that inflammation is also associated with prostate cancer (3). The source of intraprostatic inflammation is, however, largely unknown, although multiple factors, such as infectious agents, dietary carcinogens, hormone change, and physical trauma, may contribute to inflammation in the prostate gland. Chronic inflammation results in a sustained innate immune response, which creates

Requests for reprints: Shan Lu, Department of Pathology, Genome Research Institute, University of Cincinnati College of Medicine, Building A, Room 259, 2120 East Galbraith Road, Cincinnati, OH 45237-0507. Phone: 513-558-5109; Fax: 513-558-1312; E-mail: shan.lu@uc.edu.

Note: Supplementary data for this article are available at Cancer Research Online (http://cancerres.aacrjournals.org/).

Disclosure of Potential Conflicts of Interest
No potential conflicts of interest were disclosed.

microenvironment rich in cytokines, chemokines, growth factors, and angiogenesis factors, and fosters proliferation and survival, critical step for carcinogenesis (1,2). Nuclear factor κB (NF-κB) is key linking molecule in inflammation and immunity to cancer development and progression (4,5). Various carcinogens, onco genes, and cell signaling pathways, such as phosphatidylinositol 3-kinase (PI3K)-Akt signaling (6–8), activate NF-κB, which in leads to expression of inflammatory cytokines and growth factors; blocking of apoptosis; and promotion of proliferation, angiogenesis, and tumor invasion process.

Vav3 family oncogenes have three members (Vav1, Vav2, Vav3) and are guanine nucleotide exchange factors for Rho family GTPases. They differ in their tissue distributions. Vav1 is primarily expressed in hematopoietic cells, whereas Vav2 and Vav3 are more ubiquitously expressed (9,10). Vav proteins contain multiple function motifs and are involved in various cellular signaling processes including cytoskeleton organization, calcium influx, phagocytosis, and cell transformation (11). Vav proteins are directly or indirectly activated by receptor protein tyrosine kinase various signal transduction pathways. For instance, Vav2 and can be directly activated by the receptor protein tyrosine kinase activity of EphA receptor and epidermal growth factor receptor (EGFR; refs. 12,13). Vav3, a downstream signal transducer of EGFR/HER2, was shown to bind to several partners, including Rac1, Cdc42, PI3K, Grb2, and phospholipase Cγ, leading to alteration cell morphology and cell transformation (14). Overexpression Vav3 leads to PI3K activation and focus formation in NH3T3 cells, and blocking PI3K activity by PTEN and LY294002 efficiently inhibits Vav3-induced cell transformation activity (15).

Androgen receptor (AR) hypersensitivity plays a critical role prostate cancer development and progression to an androgen-independent disease. AR mutation and gene amplification, as as overexpression of coactivators, contribute to AR hypersensitivity (16–18). AR, as other nuclear receptors, can also be activated independent of its ligand by phosphorylation, which is mediated a variety of signaling pathways (19–21). Phosphorylation of facilitates the recruitment of coactivators and chromatin remodelers and modifiers, resulting in enhanced expression of its target genes (22). Numerous studies have shown that the EGFR/HER2-PI3K-Akt pathway contributes to AR hypersensitivity and prostate cancer development and progression. Overexpression of HER2 prostate cancer cells up-regulates AR activity and stimulates androgen-independent growth in prostate cancer cells (23). elevated AR activity and PI3K-Akt signaling, such as mediated PTEN deletion and mutation, play an important role in prostate cancer (24–28). Prostate-specific deletion of murine PTEN, a tumor suppressor gene that shuts off PI3K-Akt signaling, induces prostatic intraepithelial neoplasia lesions, which later progress to invasive prostate cancer in mice (29). Multiple growth factors and cytokines, including EGF, signal through the PI3K-Akt pathway and activate AR in prostate cancer cells, which can be accomplished by direct AR phosphorylation by active Akt (19–21).

Recently, we and others found that Vav3 oncogene is overexpressed in human prostate cancer and several lines of prostate cancer cells (30,31). Vav3 enhances AR activity and stimulates androgen-independent growth in prostate cancer cells. We further showed that Vav3, as a signal transducer, up-regulates AR activity partially via PI3K-Akt signaling (30). These findings suggest that Vav3 overexpression may contribute to prostate cancer development and/or progression. The purpose of this study was to further determine the role of Vav3 in prostate cancer in genetically engineered mouse model. We found that the targeted overexpression of a constitutive active Vav3 in the epithelium of the prostate gland induced prostatic intraepithelial neoplasia (mPIN) and prostate cancer, which is correlated with elevated AR signaling axis and PI3K-Akt signaling in the prostate gland. Moreover, we found that Vav3 overexpression also led to significant chronic nonbacterial inflammation in the prostate gland, which was associated with elevated incidence of prostate cancer. DNA microarray and signaling pathway analysis revealed that the top diseases and disorders are inflammatory

diseases and cancer of the prostate gland in Vav3 transgenic mice. Furthermore, we showed that overexpression of Vav3 up-regulated NF-κB activity in prostate cancer cells, which was partially via PI3K-Akt signaling. These data suggest that Vav3 overexpression enhances both the AR signaling axis and NF-κB–mediated pathway, which may contribute to the development of nonbacterial prostatitis and prostate cancer.

Materials and Methods

Reagents

RPMI 1640 was purchased from Invitrogen. Fetal bovine serum (FBS) and charcoal/dextran–treated FBS were purchased from HyClone Laboratories. Human prostate cancer LNCaP cells were obtained from American Type Culture Collection and maintained in RPMI 1640 supplemented with 10% FBS (complete medium) at 37°C in 5% CO_2. NF-κB-Luc (Clontech) is a luciferase reporter construct driven by NF-κB enhancer element.

Anti-AR and anti-Vav3 antibodies were obtained from Upstate Biotechnology. We also generated custom anti-Vav3 antibody from the COOH terminus of Vav3 peptide sequence (CMELVEYYKHHSLKEGFRT), which was used for expression analysis of transgenic Vav3* protein for the prostate tissue extracts derived from Vav3 transgenic mice. Anti–p-Akt and anti-Akt antibodies were from Cell Signaling Technology. Anti-synaptophysin polyclonal antibody was obtained from DAKO. Anti-laminin polyclonal antibody and PS-1145 were from Sigma. Anti–NF-κB antibody was purchased from Santa Cruz Biotechnology, Inc.

Generation of Vav3 transgenic mice

We generated Vav3 transgenic construct ARR_2PB-Vav3*-IRES-hrGFP. The vector backbone including a terminal intron and exon structure, mRNA termination, cleavage, and polyadenylation sequences is from SK-PB/SV40t vector, a gift from Dr. Norman Greenberg (Clinical Research, Fred Hutchinson Cancer Research Center. Seattle, WA; ref. 32). IRES containing an internal ribosome entry site and hrGFP including *Renilla* green fluorescent protein (GFP) gene were from Vitality mammalian expression vector (Stratagene). Vav3* cDNA has previously been described (30). The rat prostate-specific probasin promoter ARR_2PB was a generous gift from Dr. Robert Matusik (Director of the Vanderbilt Prostate Cancer Center, Department of Urologic Surgery, Vanderbilt University Medical Center; ref. 33). ARR_2PB is a small composite probasin promoter, which remains highly specific for the prostatic epithelium and confers a high level of transgene expression.

For genotyping of Vav3 transgenic mice by PCR, the upper primer pS5 (5′-GATTAATTAATAGCAATTCCTCGACGA-3′) and the lower primer Lw3 (5′-CTGGCCTCTCTGGCCATTATCATCGTGTTT-3′) are designed from vector IRES sequence.

Western blot analysis

Western blot analysis was done as previously described (34). Briefly, aliquots of samples with the same amount of protein, determined using the Bradford assay (Bio-Rad), were mixed with loading buffer [final concentrations of 62.5 mmol/L Tris-HCl, pH 6.8, 2.3% SDS, 100 mmol/L DTT, and 0.005% bromophenol blue], boiled, fractionated in a SDS-PAGE, and transferred onto a 0.45-μm nitrocellulose membrane (Bio-Rad). The filters were blocked with 2% fat-free milk in PBS and probed with first antibody in PBS containing 0.1% Tween 20 (PBST) and 1% fat-free milk. The membranes were then washed four times in PBST and incubated with horseradish peroxidase–conjugated secondary antibody (Bio-Rad) in PBST containing 1% fat-free milk. After washing four times in PBST, the membranes were visualized with the enhanced

chemiluminescence Western blotting detection system (Amersham Co.). For Western blot analysis of Vav3 expression, the first antibody was incubated overnight at 4°C.

Reporter assay

Cells (10^5 per well) were seeded in 12-well tissue culture plates. The next day, Optifect-mediated transfection was used for the transient transfection assay according to the protocol provided by Invitrogen/Life Technologies, Inc. The cells were then treated with hormone or drugs in stripped medium for 24 h. Subsequently, the cell extracts were prepared and luciferase activity was assessed in a Berthold Detection System (Pforzheim) using a kit from Promega following the manufacturer's instruction. For each assay, cell extract (20 μL) was used and the reaction was started by injection of 50 μL of luciferase substrate. Each reaction was measured for 10 s in a luminometer. Luciferase activity was defined as light units per milligram of protein.

Immunohistochemical staining

Immunohistochemical staining was done as detailed in our previous studies (30). Briefly, paraffin-embedded tissue sections were deparaffinized in xylene, rehydrated in graded alcohol, and transferred to PBS. The slides were treated with a citric acid–based antigen retrieval buffer (DAKO Co.), followed by 3% H_2O_2 in methanol, incubated in blocking buffer (5% bovine serum albumin and 5% horse serum in PBS) and then in the blocking buffer containing first antibody. After washing, the slides were incubated with a biotinylated secondary antibody (BioGenex Laboratories), followed by washing and incubation with the streptavidin-conjugated peroxidase (BioGenex). A positive reaction was visualized by incubating the slides with stable diaminobenzidine and counterstaining with Gill's hematoxylin (BioGenex) and mounted with Universal Mount mounting medium (Fisher Scientific).

DNA microarray analysis of the prostate glands from Vav3 transgenic mice

DNA microarray analysis was done in Genomics and Microarray Laboratory, Department of Environmental Health, University of Cincinnati Medical Center. The mouse 70-mer MEEBO oligonucleotide library version 1.05 (35,302 optimized mouse oligos; Invitrogen) was included in the DNA microarray. A pair of RNA samples from wild-type and transgenic mice was subjected to target labeling with monofunctional reactive Cy3 and Cy5 dyes (Amersham), respectively, and used per slide. Three parallel experiments were done.

Imaging and data generation were carried out with a GenePix 4000A and GenePix 4000B (Axon Instruments, Inc.) and associated software from Axon Instruments. The microarray slides were scanned with dual lasers with wavelength frequencies to excite Cy3 and Cy5 fluorescence emittance. Images were captured in JPEG and TIFF files, and DNA spots were captured by the adaptive circle segmentation method. Information extraction for a given spot is based on the median value for the signal pixels and the median value for the background pixels to produce a gene set data file for all the DNA spots. The Cy3 and Cy5 fluorescence signal intensities were normalized.

For data normalization and analysis, the data were analyzed to identify differentially expressed genes between transgenic and wild-type mice. Three biological replicate arrays, including one dye-flip, were done. Analysis was done using R statistical software and the Limma Bioconductor package (35). Data normalization was done in two steps for each microarray separately (36). First, background-adjusted intensities were log transformed and the differences (M) and averages (A) of log-transformed values were calculated as $M = \log 2(\times 1) - \log 2(\times 2)$ and $A = [\log 2(\times 1) + \log 2(\times 2)]/2$, where ×1 and ×2 denote the Cy5 and Cy3 intensities, respectively. Second, normalization was done by fitting the array-specific local regression model of M as a function of A. Normalized log-intensities for the two channels were then calculated by adding half of the normalized ratio to A for the Cy5 channel and subtracting half

of the normalized ratio from *A* for the Cy3 channel. The statistical analysis was done for each gene separately by fitting the following ANOVA model: $Y_{ijk} = m + A_i + S_j + C_k + e_{ijk}$, where Y_{ijk} corresponds to the normalized log-intensity on the *i*th array, with the *j*th genotype, and labeled with the *k*th dye ($k = 1$ for Cy5 and $k = 2$ for Cy3). m is the overall mean log-intensity, A_i is the effect of the *i*th array, S_j is the effect of the *j*th treatment, and C_k is the gene-specific effect of the *k*th dye. Estimated fold changes were calculated from the ANOVA models, and resulting *t* statistics from each comparison were modified using an intensity-based empirical Bayes method (IBMT; ref. 37).

Ingenuity Pathway Analysis

Data from oligo DNA array were analyzed through the use of Ingenuity Pathways Analysis (Ingenuity Systems).[4] Ingenuity Pathways Analysis is a software application that enables to identify the biological mechanisms, pathways, and functions most relevant to their experimental data sets or genes of interest.

For network generation and functional analysis, a data set containing gene identifiers and corresponding expression values was uploaded into the application. Each gene identifier was mapped to its corresponding gene object in the Ingenuity Pathways Knowledge Base. The gene value with >1.5-fold change and $P < 0.05$ were set to identify genes whose expression was significantly differentially regulated. Six hundred fifty-two genes were identified for pathway and 705 genes were identified for network. These genes, called focus genes, were overlaid onto a global molecular network developed from information contained in the Ingenuity Pathways Knowledge Base. Networks of these focus genes were then algorithmically generated based on their connectivity. The functional analysis of a network identified the biological functions and/or diseases that were most significant to the genes in the network. The network genes associated with biological functions and/or diseases in the Ingenuity Pathways Knowledge Base were considered for the analysis. Fisher's exact test was used to calculate a *P* value determining the probability that each biological function and/or disease assigned to that network is due to chance alone.

A network is a graphical representation of the molecular relationships between genes or gene products. Genes or gene products are represented as nodes, and the biological relationship between two nodes is represented as an edge (line). All edges are supported by at least one reference from the literature, from a textbook, or from canonical information stored in the Ingenuity Pathways Knowledge Base. The node color indicates up-regulation (*red*) or down-regulation (*green*). Nodes are displayed using various shapes that represent the functional class of the gene product.

For canonical pathway analysis of entire data set, canonical pathway analysis identified the pathways from the Ingenuity Pathways Analysis library of canonical pathways that were most significant to the data set. Genes from the data set were associated with a canonical pathway in the Ingenuity Pathways Knowledge Base and were considered for the analysis. The significance of the association between the data set and the canonical pathway was measured in two ways: (*a*) A ratio of the number of genes from the data set that map to the pathway divided by the total number of genes that map to the canonical pathway is displayed; (*b*) Fisher's exact test was used to calculate a *P* value determining the probability that the association between the genes in the data set and the canonical pathway is explained by chance alone.

[4] http://www.ingenuity.com

Real-time reverse transcription-PCR analyses

Total RNA was isolated from the prostate tissues using the TRI reagent kit (Invitrogen). For real-time reverse transcription-PCR (RT-PCR), 2 μg of total RNA were reversely transcribed at 42°C in a 20-μL reaction buffer containing 200 units of reverse transcriptase (Stratagene), 500 ng of Oligo d(T) primer, and 500 nmol/L deoxynucleotide triphosphate mix. The cDNA obtained (25 ng/reaction) was amplified in a Smart Cycler II (Cepheid) in a PCR reaction containing the primer pairs for amplification of Vav3 or β-actin and the Brilliant SYBR Green QPCR Master Mix (Stratagene). After an initial step at 95°C for 10 min, temperature cycling was started (denaturation at 95°C for 15 s, hybridization at 60°C for 15 s, and elongation at 72°C for 30 s) for 40 cycles. The cycle threshold values were used to calculate the normalized expression of Vav3 against β-actin using the Q-Gene software.

Results

Generation of Vav3 transgenic mice

We constructed ARR_2PB-Vav3*-IRES-hrGFP expression plasmid containing a constitutive active Vav3* and a downstream GFP cDNAs (Fig. 1*A*). Expression of the cDNA was confirmed by elevated GFP level in response to dehydrotestosterone stimulation in LNCaP cells. Then, the expression cassette ARR_2PB-Vav3*-IRES-hrGFP was released with *Bss*HII digestion and used to generate prostate epithelium–specific Vav3 transgenic mice in FVB genetic background. Several lines of Vav3 transgene mice were obtained (Fig. 1*B*). Expression of the transgene, a 75-kDa Vav3* protein (30), was confirmed in tissue extracts derived from the prostate gland of 8-week-old mice (Fig. 1*C*). Immunohistochemistry analysis revealed that Vav3 protein was overexpressed in the prostate epithelium at this age (Fig. 1*D*).

Development of mPIN and prostate cancer in Vav3 transgenic mice

The prostate glands from three lines of Vav3 transgenic mice of ages 2 to 10 months were collected and subjected to H&E staining. The abnormality in the prostate gland tissue was observed in Vav3 transgenic mice, dramatically in young adult mice relative to wild-type mice. Histopathologic analysis revealed that some of the transgenic mice developed prostate cancer (Table 1). As shown in Fig. 2, the prostate glands from Vav3 transgenic mice of age 6 months developed mPIN and prostate cancer. The glandular epithelium showed prominent proliferation, with glands varying in size and shape with mixed and different epithelium growth patterns (tufted, papillary, or cribriform as indicated by arrow; Fig. 2*B*). The epithelial cells showed high-grade cellular atypia with amphophilic to basophilic cytoplasm and prominent stratification and crowding of nuclei. The nuclei were enlarged and hyperchromatic with coarse clumping of chromatin, prominent nucleoli, and irregular nuclear membrane (Fig. 2*B-III*, *inset*). Microinvasion presented in focal area lacking a basal cell layer and with glands invading the surrounding stroma (Fig. 2*B-IV*). No distant metastasis was identified. Table 1*A* summarizes the results of 85 transgenic mice from 3 transgenic lines and 17 wild-type mice. The equality of cancer rates in transgenic mice and wild-type mice was tested by Fisher's exact test after collapsing the age groups. When wild-type and mPIN mice were combined as noncancer cases, the cancer rate in transgenic mice was found significantly higher than that in wild-type mice ($P < 0.001$).

Lymphomononuclear cell infiltration in the prostate glands of Vav3 transgenic mice

A further analysis revealed the presence of significant inflammatory responses in prostate glands of Vav3 transgenic mice. Lymphomononuclear cells were mostly notable in the stroma of prostate glands and consisted mainly of lymphocytes, plasma cells, and monocytes (Fig. 3*A*–*C*; refs. 38, 39). The predominance of lymphocytes and plasma cells indicated a chronic inflammatory process. The lack of or rare presence of neutrophils was also supported that this

inflammation was not an acute inflammatory process, which is usually caused by bacterial infection. More interestingly, there was a notable angiogenesis that seemed to be associated with the inflammatory process (Fig. 3*D*).

These observations prompted us to investigate whether inflammation was associated with prostate cancer development in Vav3 transgenic mice. We analyzed one line of Vav3 transgenic mice of ages 5 to 7 months. Among 11 mice with prostate cancer, 8 (73%) mice had significant inflammation in the prostate gland, whereas 2 of 13 (15%) wild-type mice showed minimum inflammatory cell infiltration. Furthermore, we found that the onset of inflammation in the prostate gland is approximately the same time as the neoplastic changes, which is at ages 5 to 6 months. Statistical analysis by Fisher's exact tests suggested that there is a significant association of inflammation and prostate cancer development ($P = 0.011$). These data suggest that inflammatory responses are associated with prostate cancer development in Vav3 transgenic mice.

Characterization of prostate cancer in Vav3 transgenic mice

We characterized prostate cancer in Vav3 transgenic mice and examined the expression levels of Vav3 and AR in the prostate glands of 6-month-old mice. Immunohistochemical analysis revealed that Vav3 expression was elevated in the prostate epithelial cells of Vav3 transgenic mice relative to those of wild-type mice (Fig. 4*A*). The prostate epithelial cells were positive for AR staining. There was no significant alteration in AR protein level between Vav3 transgenic and wild-type mice based on Western blot analysis (Fig. 4*A*). Laminin staining showed the disruption of the basal cell layer in the prostate glands of Vav3 transgenic mice, whereas the glandular structure was intact in wild-type mice of the same age. These data indicate a local invasive prostate cancer in Vav3 transgenic mice. α-Synaptophysin staining was negative in epithelial cells and positive in neuronal cells of the stroma, suggesting that the prostate cancer cells were not of neuroendocrine origin (Fig. 4*A*).

PI3K-Akt signaling was elevated in the prostate epithelium

Given our previous finding that Vav3 overexpression enhances AR signaling partially via the PI3K-Akt pathway (30), we examined PI3K-Akt signaling in the prostate gland of Vav3 transgenic mice. Immunohistochemical analysis showed that phospho-Akt level was elevated in the prostate epithelial cells of Vav3 transgenic mice relative to those in wild-type mice (Fig. 4*B*). Western blot analysis confirmed that phospho-Akt level was elevated in the tissue extracts derived from the prostate gland of Vav3 transgenic mice compared with those of wild-type mice (Fig. 4*C*). This finding is consistent with our previous *in vitro* data indicating that Vav3 enhances PI3K-Akt signaling (30).

The AR signaling axis was elevated in the prostate epithelium

To further determine alterations of the signaling pathways in the prostate glands of Vav3 transgenic mice, we conducted DNA microarray analysis using RNAs derived from the prostate glands of Vav3 transgenic mice. The expression of genes in the prostate glands of Vav3 transgenic mice was compared with that in age-matched wild-type mice. The initial analysis was focused on the AR-mediated pathways. Data in Table 1*B* showed that Vav3 overexpression enhanced the AR signaling axis as shown by enhanced expression of AR target genes as well as AR signaling–related genes. The levels of kallikrein 1 and sex-limited protein genes, which are classic AR target genes, were elevated. The levels of androgen binding proteins/sex hormone–binding globulins were also increased, which are involved in extracellular steroid binding and bioavailability of sex steroids. In addition, expression of caveolin 1, which is involved in nongenomic AR activity and prostate cancer, was elevated. We validated the microarray data by quantitative real-time RT-PCR and found that murine KLK-1 level was ~2.8-fold higher in the prostate glands of Vav3 transgenic mice (3.33e–4 relative to Actin

mRNA level) compared with wild-type mice (1.2e–4 relative to actin mRNA level). These data strongly suggest that Vav3 overexpression enhanced the AR signaling axis, which could be one of the mechanisms by which overexpression of Vav3 induced the development of prostate cancer.

Determination of the disrupted signaling pathways in the prostate glands of Vav3 transgenic mice

To identify the alterations of other signaling pathways in Vav3 transgenic mice, the DNA microarray data were subjected to Ingenuity Pathway Analysis. Genes that have expression levels changed >1.5-fold and $P < 0.05$ were chosen for analysis. Under these criteria, 652 genes qualified for pathway analysis and 705 genes for network analysis. Consistent with cancer and inflammation phenotypes in the prostate glands of Vav3 transgenic mice, the top diseases and disorders identified by Ingenuity Pathway Analysis were cancer and inflammatory disease with $P = 4.36e{-}12$ and $P = 4.58e{-}13$, respectively. The genes related to prostate cancer and inflammation were listed in Supplementary Tables S1 and S2. Furthermore, Ingenuity Pathway Analysis identified 68 networks, among which 36 networks were overlapping. On the top of the list in identified networks were cancer and inflammation networks, which overlapped with each other (Fig. 5*A*; high-magnification images of Fig. 5*A* were shown in Supplementary Figs. S1–S3; the genes in the networks were listed in Supplementary Table S3). In addition, expression levels of a series of inflammation-related genes in the NF-κB–mediated pathway, including chemokines, cytokines, growth factors, and their receptors, were elevated (Supplementary Table S4). Expression levels of NF-κB–regulated genes, such as *Bfl1/A1* and *VEGF*, are also enhanced. Because prostate cancer is heterogeneous and of epithelial origin and total RNA for DNA microarray is from whole prostate gland including stroma, there is potential that many genes overexpressing in the prostate cancer cells fail to be detected by DNA microarray analysis or do not pass statistical significance. We validated the DNA microarray data by quantitative real-time RT-PCR and found that the expression levels of murine proinflammatory cytokines interleukin (IL)-6 and KC, a murine homologue of human IL-8 (40), were ~2.6- and 4.8-fold higher in the prostate glands of Vav3 transgenic mice (8.1e–5 and 24.1e–4 relative to actin mRNA level) compared with those of wild-type mice (3.1e–5 and 4.97e–4 relative to actin mRNA level), respectively. These analyses confirmed the tumorigenic effects of Vav3 overexpression leading to prostate cancer at the molecular level. Moreover, data from these studies supported the inflammation phenotype observed in the prostate glands of Vav3 transgenic mice (Fig. 3) and showed at the molecular level that enhanced Vav3 function also resulted in inflammatory disease in the prostate gland.

Vav3 up-regulated NF-κB signaling

It has been shown that PI3K-Akt signaling up-regulates the NF-κB–mediated pathway, which in turn plays critical roles in inflammatory responses (6–8). In addition, it was reported that there is an increased NF-κB expression and activity in prostate cancer, which is correlated with the disease progression (41,42). We examined whether there is an increased NF-κB level and nucleus localization in the prostate epithelial cells of Vav3 transgenic mice by immunohistochemical analysis. We found that the level of NF-κB/p65 (Rel A) is increased in the prostatic epithelial cells and also moderately elevated in the nucleus of the cells of Vav3 transgenic mice in comparison with those of wild-type mice (Fig. 5*B*).

We then determined whether Vav3 regulates NF-κB activity via PI3K-Akt signaling in a reporter assay. LNCaP cells were transiently cotransfected with luciferase reporter NF-κB-Luc and expression vector for Vav3 or constitutive active Vav3*. The cells were then treated with EGF, PI3K inhibitor LY294002, or epidermal growth factor (EGF) plus LY294002. As shown in Fig. 5*C*, overexpression of Vav3 elevated basal NF-κB activity in LNCaP cells. EGF-stimulated NF-κB activity was further enhanced by overexpressing Vav3. Vav3-enhanced NF-

κB activity was inhibited by treatment with LY294002. EGF stimulation partially attenuated the inhibitory effects of LY294002 on Vav3-induced NF-κB activation. The stimulatory effect on NF-κB activity was more evident in cells transfected with Vav3* and Vav3* plus EGF stimulation (Fig. 5*C*). In addition, overexpression of Vav3*, relative to Vav3, compromised the inhibitory effect for NF-κB by LY294002. Furthermore, we confirmed whether Vav3 regulates NF-κB activity mediated by NF-κB. LNCaP cells were transiently cotransfected with luciferase reporter NF-κB-Luc and Vav3* expression vector. The cells were then treated with EGF in the absence or presence of the IκB kinase inhibitor PS-1145 (43). We found that blocking the activity of IκB kinase, an upstream kinase essential for NF-κB activation, significantly compromised NF-κB activity stimulated by Vav3 and EGF (Fig. 5*D*). These data indicated that Vav3 overexpression enhances NF-κB activity, which is at least partially mediated by PI3K-Akt signaling.

Discussion

Our previous study showed that Vav3 is overexpressed in human prostate cancer, stimulates prostate cancer cell growth, and enhances the AR signaling axis partially via the PI3K-Akt pathway (30), suggesting a potential role of Vav3 in prostate cancer. Data presented in the present study confirm and extend these observations. Indeed, the AR-mediated signaling axis and PI3K-Akt signaling are elevated in the prostate gland of Vav3 transgenic mice, a genetically engineered prostate cancer model. Vav3 transgenic mice develop mPIN and prostate cancer in young adult mice. However, we did not observe a distant metastasis in the transgenic mice, suggesting that additional factors are required for this phenotype. Some Vav3 transgenic mice develop a significant inflammatory response and angiogenesis in the prostate gland, which is associated with the elevated incidence of prostate cancer. These findings are supported by data from DNA microarray and signaling pathway analysis, showing that inflammatory diseases and cancer of the prostate gland in Vav3 transgenic mice are among the top disorders. Moreover, we found that Vav3 overexpression up-regulates NF-κB–mediated signaling at least partially via PI3K-Akt signaling, implicating an underlying mechanism of inflammatory response in the prostate glands of Vav3 transgenic mice.

Vav proteins are signal transducers of receptor protein tyrosine kinase in various signal transduction pathways. Vav3 can be activated by the receptor protein tyrosine kinase activity of EphA receptor and EGFR, and in turn, Vav3 signals downstream through the PI3K-Akt pathway (12–15). It has been well documented that elevated signaling of the EGFR/HER2-PI3K-Akt pathway contributes to AR hypersensitivity and prostate cancer. We showed in our Vav3 transgenic model that Vav3 overexpression enhances the signaling levels of both the PI3K-Akt pathway and AR signaling axis, which may contribute to prostate cancer development. However, the molecular mechanism of Vav3 action in the context of the EGFR/HER2-PI3K-Akt pathway and AR signaling axis remains to be determined.

Inflammation, when it runs unchecked, can also lead to a host of diseases, such as hay fever, atherosclerosis, and rheumatoid arthritis. Chronic inflammation is a pathologic condition characterized by concurrent active inflammation, tissue destruction, and attempts at repair. Chronically inflamed tissue shows the infiltration of lymphomononuclear immune cells (monocytes, macrophages, lymphocytes, and plasma cells), tissue destruction, and attempts at healing, which include angiogenesis and fibrosis (44). Histopathologically, inflammation is associated with prostate cancer (3). In our genetically engineered mouse prostate cancer model, we found that lymphomononuclear cell infiltration in the prostate gland mainly consists of monocytes, lymphocytes, and plasma cells, but lacks neutrophils, suggesting that the inflammation is not due to bacterial infection (39,45). Significantly, the presence of plasma cells indicates chronic inflammation (44). More significantly, we found that inflammation is associated with prostate cancer development.

NIH category I and II prostatitis are acute and chronic prostatitis caused by bacterial infection (46,47). However, the etiology of category III and IV prostatitis is not clear. Category III prostatitis, chronic prostatitis/chronic pelvic pain syndrome (CP/CPPS), is a poorly understood disorder, even though it accounts for 90% to 95% of prostatitis diagnosed (48). Theories behind the disease include autoimmunity. CP/CPPS may be inflammatory (category IIIa) or noninflammatory (category IIIb), whereas both categories show evidence of inflammation (49,50). Category IV prostatitis is asymptomatic inflammatory prostatitis (51). These patients have no history of genitourinary pain complaints, but leukocytosis is noted, usually during evaluation for other conditions. Asymptomatic prostatic inflammation may sometimes be associated with prostate cancer. Our Vav3 transgenic mice develop nonbacterial chronic prostatitis, which is induced by overexpression of Vav3 oncogene. This is the first prostatitis model induced by genetic factor, suggesting a novel mechanism of prostatitis.

It has been shown that PI3K-Akt signaling activates NF-κB (6–8). It has been well documented that NF-κB activation leads to expression of inflammatory cytokine and growth factors, blocking of apoptosis, promotion of proliferation, angiogenesis, and tumor invasion process. It was also reported that there is an increased NF-κB expression and activity in prostate cancer, which is correlated with the disease progression (41,42). In the current study, we showed that Vav3 enhances PI3K-Akt signaling (30). We also found that Vav3 overexpression enhances NF-κB–mediated signaling partially via the PI3K-Akt pathway (4,5). We observed an elevated angiogenesis in the prostate glands from Vav3 transgenic mice. Consistently, DNA microarray analysis revealed that expression levels of a series of inflammation-related genes in the NF-κB–mediated pathway, including chemokines, cytokines, growth factors, and their receptors, were elevated. This finding suggests that genetic alteration by Vav3 overexpression aberrantly stimulates innate immune response, leading to inflammation in the prostate gland. NF-κB may be a key linking molecule in Vav3-induced inflammation, which is associated with prostate cancer development.

Among genetically engineered mouse prostate cancer models induced by a single endogenous gene, PTEN null mice, generated by prostatic epithelial cell-specific PTEN knockout, develop mPIN, prostate cancer, and distant metastasis (29,52). Overexpression of c-myc oncogene in the prostate gland induces locally invasive adenocarcinoma without distant metastasis (53). Here we report that prostatic epithelium–specific Vav3 transgenic mice develop nonbacterial prostatitis and prostate cancer. Vav3*, a Vav3 mutant with NH_2-terminal domain deletion, is a constitutive active form and has very strong oncogenic effect compared with wild-type Vav3 (54). This study proves a principle that enhancement of single Vav3 gene function leads to prostatitis and prostate cancer development, suggesting an important role of the Vav3-mediated pathway in prostate cancer biology.

In summary, our Vav3 transgenic mice, a genetically engineered mouse prostatitis and prostate cancer model, showed that elevated Vav3 function leads to enhanced signaling levels in both NF-κB–and AR-mediated pathways, partially via PI3K-Akt signaling, and induces nonbacterial chronic inflammatory response and cancer development in the prostate gland. This study suggests that Vav3-mediated signaling plays a critical role in prostatitis and prostate cancer.

Supplementary Material

Refer to Web version on PubMed Central for supplementary material.

Acknowledgments

Grant support: Barrett Cancer Center at the University of Cincinnati College of Medicine and grants from Ohio Cancer Research Associates, NIH grants R01 CA119935 and CA97099, and American Cancer Society grant RSG-98332-02-CCE.

We thank Dr. Alex Lentsch (Department of Surgery, University of Cincinnati College of Medicine) for consultation on inflammatory responses.

References

1. Karin M, Lawrence T, Nizet V. Innate immunity gone awry: linking microbial infections to chronic inflammation and cancer. Cell 2006;124:823–35. [PubMed: 16497591]
2. Coussens LM, Werb Z. Inflammation and cancer. Nature 2002;420:860–7. [PubMed: 12490959]
3. De Marzo AM, Platz EA, Sutcliffe S, et al. Inflammation in prostate carcinogenesis. Nat Rev Cancer 2007;7:256–69. [PubMed: 17384581]
4. Karin M, Greten FR. NF-κB: linking inflammation and immunity to cancer development and progression. Nat Rev Immunol 2005;5:749–59. [PubMed: 16175180]
5. Karin M. Nuclear factor-κB in cancer development and progression. Nature 2006;441:431–6. [PubMed: 16724054]
6. Fan S, Gao M, Meng Q, et al. Role of NF-κB signaling in hepatocyte growth factor/scatter factor-mediated cell protection. Oncogene 2005;24:1749–66. [PubMed: 15688034]
7. Vandermoere F, El Yazidi-Belkoura I, Adriaenssens E, Lemoine J, Hondermarck H. The antiapoptotic effect of fibroblast growth factor-2 is mediated through nuclear factor-κB activation induced via interaction between Akt and IκB kinase-β in breast cancer cells. Oncogene 2005;24:5482–91. [PubMed: 15856005]
8. Gong L, Li Y, Nedeljkovic-Kurepa A, Sarkar FH. Inactivation of NF-κB by genistein is mediated via Akt signaling pathway in breast cancer cells. Oncogene 2003;22:4702–9. [PubMed: 12879015]
9. Bustelo XR. Regulatory and signaling properties of the Vav family. Mol Cell Biol 2000;20:1461–77. [PubMed: 10669724]
10. Bustelo XR. Vav proteins, adaptors and cell signaling. Oncogene 2001;20:6372–81. [PubMed: 11607839]
11. Katzav S, Martin-Zanca D, Barbacid M. vav, a novel human oncogene derived from a locus ubiquitously expressed in hematopoietic cells. EMBO J 1989;8:2283–90. [PubMed: 2477241]
12. Hunter SG, Zhuang G, Brantley-Sieders D, Swat W, Cowan CW, Chen J. Essential role of Vav family guanine nucleotide exchange factors in EphA receptor-mediated angiogenesis. Mol Cell Biol 2006;26:4830–42. [PubMed: 16782872]
13. Tamas P, Solti Z, Bauer P, et al. Mechanism of epidermal growth factor regulation of Vav2, a guanine nucleotide exchange factor for Rac. J Biol Chem 2003;278:5163–71. [PubMed: 12454019]
14. Zeng L, Sachdev P, Yan L, et al. Vav3 mediates receptor protein tyrosine kinase signaling, regulates GTPase activity, modulates cell morphology, and induces cell transformation. Mol Cell Biol 2000;20:9212–24. [PubMed: 11094073]
15. Sachdev P, Zeng L, Wang LH. Distinct role of phosphatidylinositol 3-kinase and Rho family GTPases in Vav3-induced cell transformation, cell motility, and morphological changes. J Biol Chem 2002;277:17638–48. [PubMed: 11884391]
16. Taplin ME, Bubley GJ, Shuster TD, et al. Mutation of the androgen-receptor gene in metastatic androgen-independent prostate cancer. N Engl J Med 1995;332:1393–8. [PubMed: 7723794]
17. Visakorpi T, Hyytinen E, Koivisto P, et al. *In vivo* amplification of the androgen receptor gene and progression of human prostate cancer. Nat Genet 1995;9:401–6. [PubMed: 7795646]
18. Zhou HJ, Yan J, Luo W, et al. SRC-3 is required for prostate cancer cell proliferation and survival. Cancer Res 2005;65:7976–83. [PubMed: 16140970]
19. Wen Y, Hu MC, Makino K, et al. HER-2/neu promotes androgen-independent survival and growth of prostate cancer cells through the Akt pathway. Cancer Res 2000;60:6841–5. [PubMed: 11156376]

20. Craft N, Shostak Y, Carey M, Sawyers CL. A mechanism for hormone-independent prostate cancer through modulation of androgen receptor signaling by the HER-2/neu tyrosine kinase. Nat Med 1999;5:280–5. [PubMed: 10086382]
21. Yeh S, Lin HK, Kang HY, Thin TH, Lin MF, Chang C. From HER2/Neu signal cascade to androgen receptor and its coactivators: a novel pathway by induction of androgen target genes through MAP kinase in prostate cancer cells. Proc Natl Acad Sci U S A 1999;96:5458–63. [PubMed: 10318905]
22. Rochette-Egly C. Nuclear receptors: integration of multiple signalling pathways through phosphorylation. Cell Signal 2003;15:355–66. [PubMed: 12618210]
23. Signoretti S, Montironi R, Manola J, et al. Her-2-neu expression and progression toward androgen independence in human prostate cancer. J Natl Cancer Inst 2000;92:1918–25. [PubMed: 11106683]
24. Whang YE, Wu X, Suzuki H, et al. Inactivation of the tumor suppressor PTEN/MMAC1 in advanced human prostate cancer through loss of expression. Proc Natl Acad Sci U S A 1998;95:5246–50. [PubMed: 9560261]
25. Cairns P, Okami K, Halachmi S, et al. Frequent inactivation of PTEN/MMAC1 in primary prostate cancer. Cancer Res 1997;57:4997–5000. [PubMed: 9371490]
26. Murillo H, Huang H, Schmidt LJ, Smith DI, Tindall DJ. Role of PI3K signaling in survival and progression of LNCaP prostate cancer cells to the androgen refractory state. Endocrinology 2001;142:4795–805. [PubMed: 11606446]
27. Vlietstra RJ, van Alewijk DC, Hermans KG, van Steenbrugge GJ, Trapman J. Frequent inactivation of PTEN in prostate cancer cell lines and xenografts. Cancer Res 1998;58:2720–3. [PubMed: 9661880]
28. Lu S, Ren CX, Liu Y, Epner DE. The PI3K-Akt signaling is involved in regulation of p21WAF/CIP expression and androgen-independent growth in prostate cancer cells. Int J Oncol 2006;28:245–51. [PubMed: 16328002]
29. Wang S, Gao J, Lei Q, et al. Prostate-specific deletion of the murine Pten tumor suppressor gene leads to metastatic prostate cancer. Cancer Cell 2003;4:209–21. [PubMed: 14522255]
30. Dong ZY, Liu Y, Lu S, et al. Vav3 oncogene is overexpressed and regulates cell growth and androgen receptor activity in human prostate cancer. Mol Endo 2006;20:2315–25.
31. Lyons LS, Burnstein KL. Vav3, a Rho GTPase guanine nucleotide exchange factor, increases during progression to androgen independence in prostate cancer cells and potentiates androgen receptor transcriptional activity. Mol Endocrinol 2006;20:1061–72. [PubMed: 16384856]
32. Gingrich JR, Barrios RJ, Morton RA, et al. Metastatic prostate cancer in a transgenic mouse. Cancer Res 1996;56:4096–102. [PubMed: 8797572]
33. Zhang J, Thomas TZ, Kasper S, Matusik RJ. A small composite probasin promoter confers high levels of prostate-specific gene expression through regulation by androgens and glucocorticoids *in vitro* and *in vivo*. Endocrinology 2000;141:4698–710. [PubMed: 11108285]
34. Lu S, Tsai SY, Tsai MJ. Melecular mechanisms of androgen-independent growth of human prostate cancer LNCaP-AI cells. Endocrinology 1999;140:5054–9. [PubMed: 10537131]
35. Smyth GK. Linear models and empirical bayes methods for assessing differential expression in microarray experiments. Stat Appl Genet Mol Biol 2004;3Article 3
36. Sartor M, Schwanekamp J, Halbleib D, et al. Microarray results improve significantly as hybridization approaches equilibrium. Biotechniques 2004;36:790–6. [PubMed: 15152598]
37. Sartor MA, Tomlinson CR, Wesselkamper SC, Sivaganesan S, Leikauf GD, Medvedovic M. Intensity-based hierarchical Bayes method improves testing for differentially expressed genes in microarray experiments. BMC Bioinformatics 2006;7:538. [PubMed: 17177995]
38. Nickel JC, True LD, Krieger JN, Berger RE, Boag AH, Young ID. Consensus development of a histopathological classification system for chronic prostatic inflammation. BJU Int 2001;87:797–805. [PubMed: 11412216]
39. Penna G, Amuchastegui S, Cossetti C, et al. Spontaneous and prostatic steroid binding protein peptide-induced autoimmune prostatitis in the non-obese diabetic mouse. J Immunol 2007;179:1559–67. [PubMed: 17641022]
40. Bozic CR, Kolakowski LF Jr, Gerard NP, et al. Expression and biologic characterization of the murine chemokine KC. J Immunol 1995;154:6048–57. [PubMed: 7751647]

41. Shukla S, MacLennan GT, Fu P, et al. Nuclear factor-κB/p65 (Rel A) is constitutively activated in human prostate adenocarcinoma and correlates with disease progression. Neoplasia 2004;6:390–400. [PubMed: 15256061]
42. Lessard L, Begin LR, Gleave ME, Mes-Masson AM, Saad F. Nuclear localisation of nuclear factor-κB transcription factors in prostate cancer: an immunohistochemical study. Br J Cancer 2005;93:1019–23. [PubMed: 16205698]
43. Domingo-Domenech J, Oliva C, Rovira A, et al. Interleukin 6, a nuclear factor-κB target, predicts resistance to docetaxel in hormone-independent prostate cancer and nuclear factor-κB inhibition by PS-1145 enhances docetaxel antitumor activity. Clin Cancer Res 2006;12:5578–86. [PubMed: 17000695]
44. Cotran, RS.; Kumar, V.; Collins, T.; Robbins, SL. Robbins pathologic basis of disease. Philadelphia: WB Saunders Company; 1999.
45. Penna G, Amuchastegui S, Cossetti C, et al. Treatment of experimental autoimmune prostatitis in nonobese diabetic mice by the vitamin D receptor agonist elocalcitol. J Immunol 2006;177:8504–11. [PubMed: 17142748]
46. Luzzi GA. Chronic prostatitis and chronic pelvic pain in men: aetiology, diagnosis and management. J Eur Acad Dermatol Venereol 2002;16:253–6. [PubMed: 12195565]
47. Habermacher GM, Chason JT, Schaeffer AJ. Prostatitis/chronic pelvic pain syndrome. Annu Rev Med 2006;57:195–206. [PubMed: 16409145]
48. Clemens JQ, Meenan RT, O'Keeffe Rosetti MC, Gao SY, Calhoun EA. Incidence and clinical characteristics of National Institutes of Health type III prostatitis in the community. J Urol 2005;174:2319–22. [PubMed: 16280832]
49. Ullrich PM, Turner JA, Ciol M, Berger R. Stress is associated with subsequent pain and disability among men with nonbacterial prostatitis/pelvic pain. Ann Behav Med 2005;30:112–8. [PubMed: 16173907]
50. Hedelin H, Jonsson K. Chronic prostatitis/chronic pelvic pain syndrome: symptoms are aggravated by cold and become less distressing with age and time. Scand J Urol Nephrol 2007;41:516–20. [PubMed: 17853027]
51. Stancik I, Luftenegger W, Klimpfinger M, Muller MM, Hoeltl W. Effect of NIH-IV prostatitis on free and free-to-total PSA. Eur Urol 2004;46:760–4. [PubMed: 15548444]
52. Kasper S. Survey of genetically engineered mouse models for prostate cancer: analyzing the molecular basis of prostate cancer development, progression, and metastasis. J Cell Biochem 2005;94:279–97. [PubMed: 15565647]
53. Ellwood-Yen K, Graeber TG, Wongvipat J, et al. Myc-driven murine prostate cancer shares molecular features with human prostate tumors. Cancer Cell 2003;4:223–38. [PubMed: 14522256]
54. Lopez-Lago M, Lee H, Cruz C, Movilla N, Bustelo XR. Tyrosine phosphorylation mediates both activation and down-modulation of the biological activity of Vav. Mol Cell Biol 2000;20:1678–91. [PubMed: 10669745]

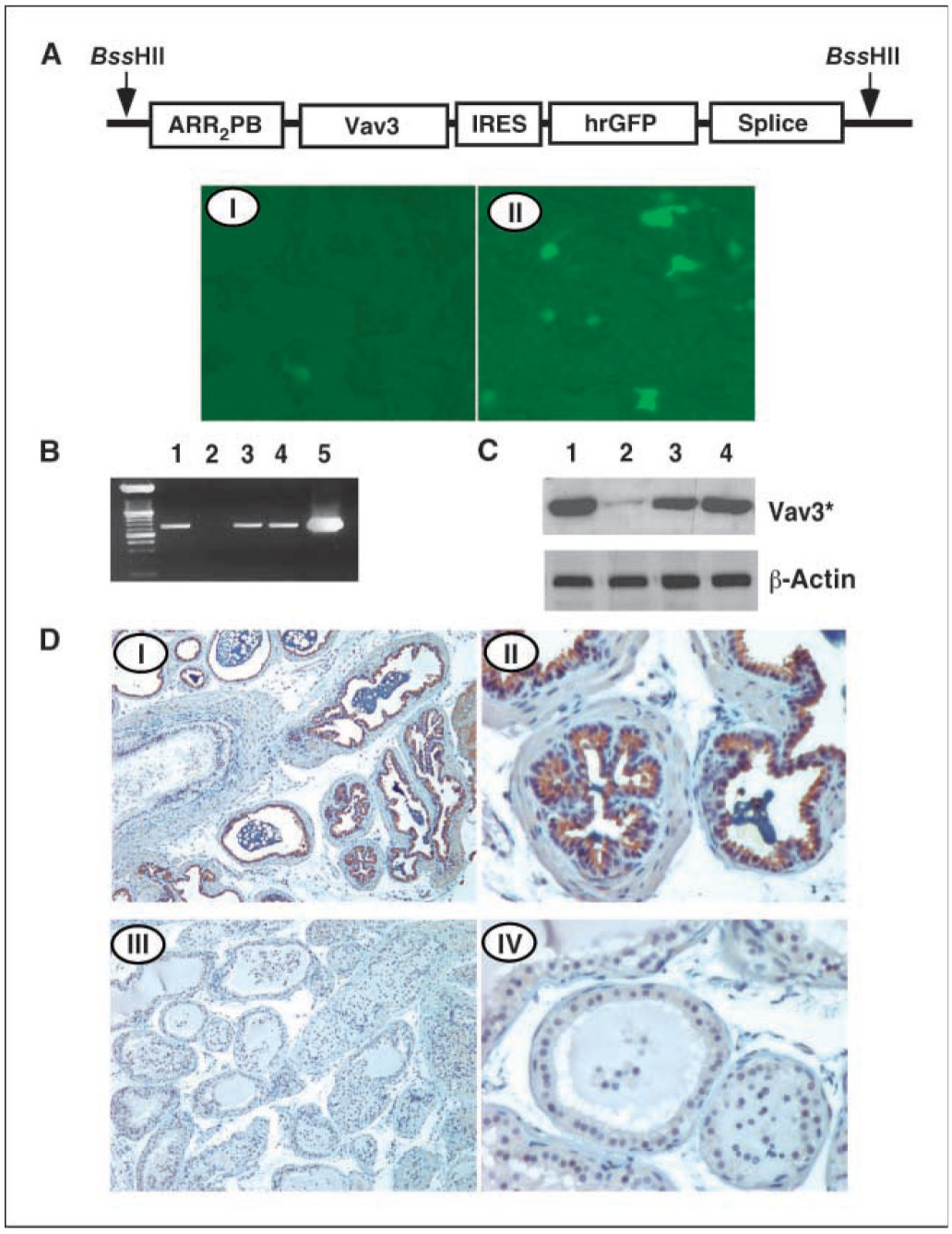

Figure 1.

Generation of Vav3 transgenic mice. *A*, construct ARR_2PB-Vav3-IRES-hrGFP. ARR_2PB is a small composite probasin promoter; Vav3 is Vav3* cDNA; IRES is an internal ribosome entry site; hrGFP is *Renilla* GFP gene. Splice includes a terminal intron and exon structure, mRNA termination, cleavage, and polyadenylation sequences. LNCaP cells were transiently transfected with ARR_2PB-Vav3-IRES-hrGFP and then cultured in stripped medium without (*I*) or with (*II*) dehydrotestosterone (10^{-8} mol/L) for 24 h. The cells were observed under a fluorescence microscope. *B*, genotyping of Vav3 transgenic mice. *Lanes 1*, *3*, and *4*, positive pups; *lane 2*, a negative pup. *Lane 5*, PCR-positive control. *C*, prostate tissue extracts from mice were subjected to Vav3* expression analysis by Western blot. *Lane 1*, *3*, and *4*, extracts

from transgenic mice; *lane 2*, extract from negative mouse. *D*, immunohistochemical analysis of Vav3 expression in the dorsal prostate glands of Vav3 transgenic mouse (*I* and *II*) and control mouse (*III* and *IV*). Magnification, ×100 (*I* and *III*); ×400 (*II* and *IV*).

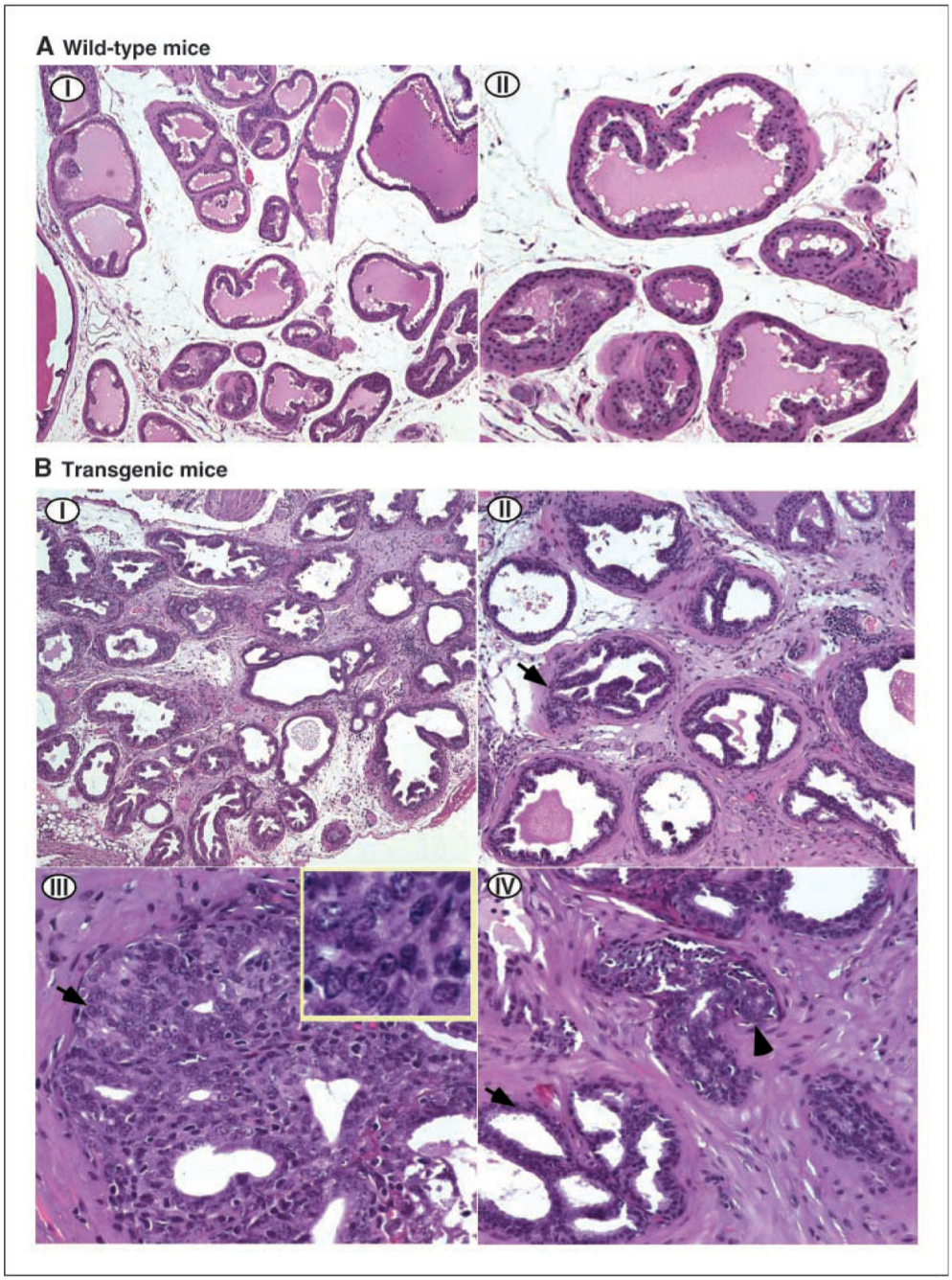

Figure 2.

Development of mPIN and prostate cancer with focal microinvasion in Vav3 transgenic mice. *A,* prostate glands from 6-month-old wild-type mice. Magnification, ×100 (*I*); ×200 (*II*). *B,* prostate glands from Vav3 transgenic mice. Low-power view (*I* and *II*) shows glandular hyperplasia with mild architectural alteration and stroma hypercellularity. Prominent proliferation of glandular epithelium with glands varying in size and shape with mixed, different growth patterns (tufted, papillary, or cribriform as indicated by *arrow*). Some glands are angulated and rigid in appearance. Other atypical features include fused glands, trabecular bar, and punched out or slit-like lumina. Under high-power view (*III*), the epithelial cells show high-grade cellular atypia with basophilic cytoplasm and prominent stratification and crowding

of nuclei. The nuclei are enlarged and hyperchromatic with coarse clumping of chromatin, prominent nucleoli, and irregular nuclear membrane. Microinvasion (*IV; arrowhead*) is present in focal area lacking a basal cell layer and with glands invading the surrounding stroma. Magnification, ×100 (*I*); ×200 (*II*); ×400 (*III*); ×600 (*inset*); and ×400 (*IV*). All sections are H&E stained.

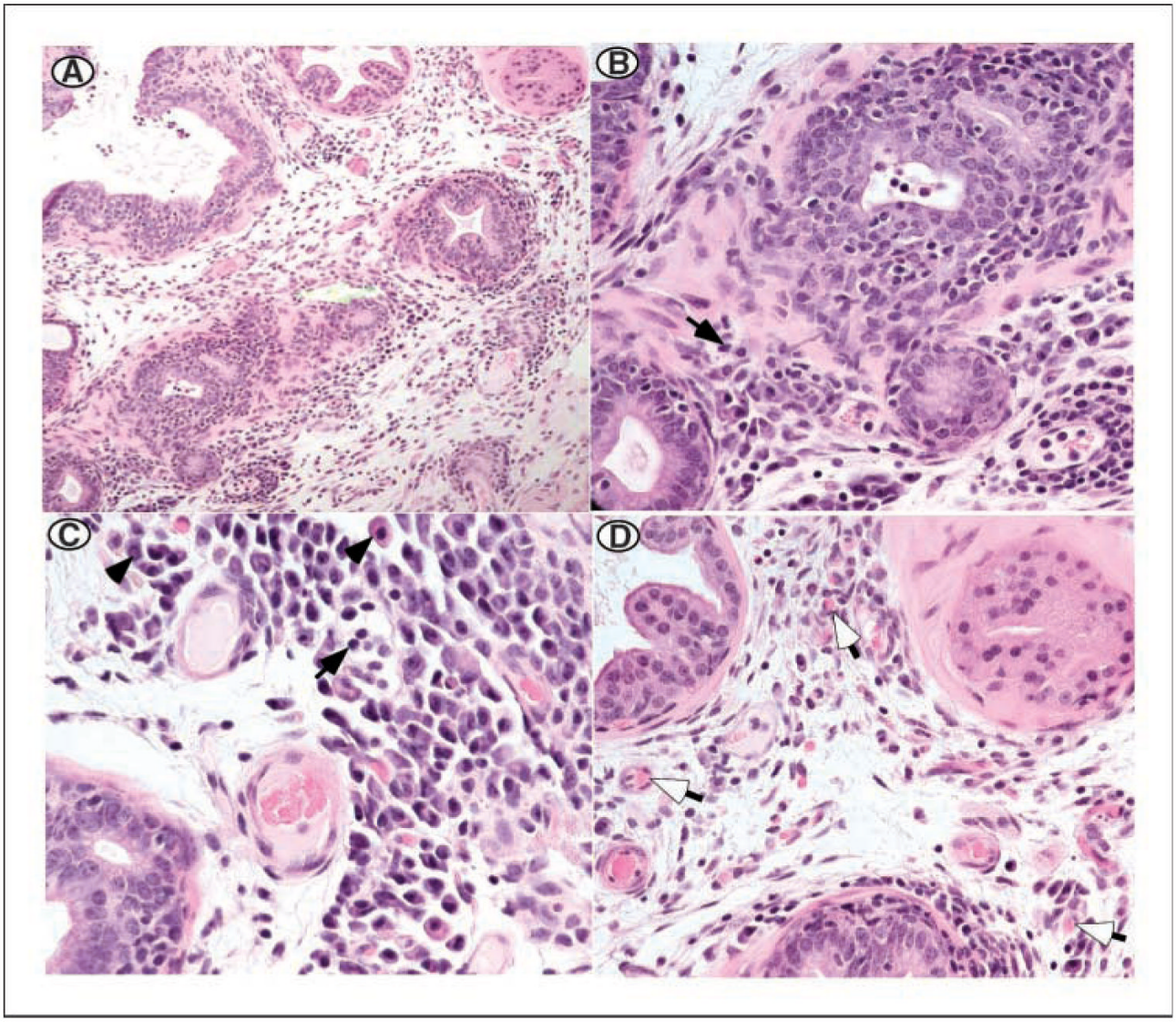

Figure 3.

Chronic lymphomononuclear cell infiltrate and significant angiogenesis in the prostate glands of Vav3 transgenic mice. *A* to *C*, the prostate gland from a 6-month-old mouse shows lymphomononuclear cell infiltrate in both glandular epithelium and stroma. The inflammatory cells consist predominantly of lymphocytes (*arrow*) and plasma cells (*arrowhead*). *D*, in addition to inflammation, there is a significant angiogenesis with new blood vessel formation (*open arrow*). All sections are H&E stained. Magnification, ×100 (*A*); ×200 (*B*); ×400 (*C*); and ×200 (*D*).

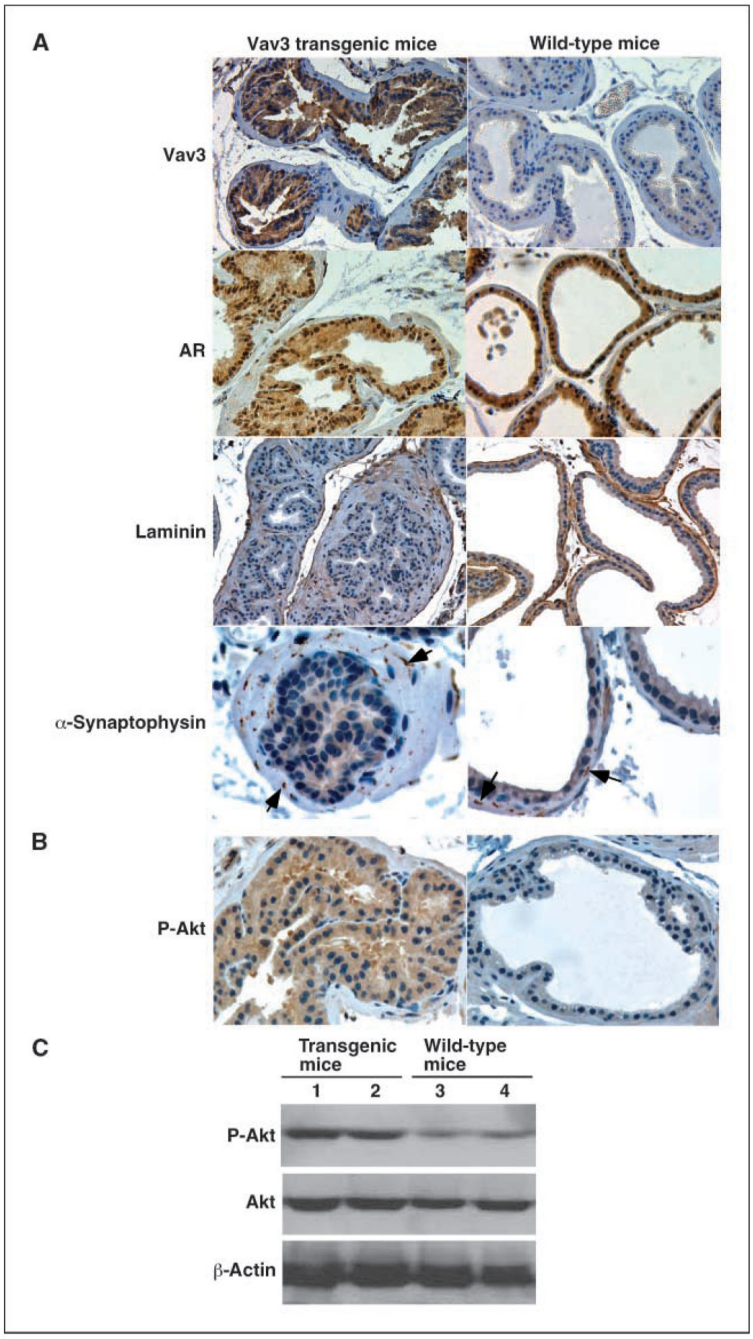

Figure 4.

Characterization of prostate cancer in Vav3 transgenic mice. *A*, immunohistochemical analysis of the prostate glands of Vav3 transgenic mice (*left*) relative to that of wild-type mice (*right*) of ages 6 mo for Vav3, AR, laminin, and α-synaptophysin. Magnification, ×200 (Vav3, AR, and laminin); ×600 (α-synaptophysin). *B*, expression analysis of phospho-Akt in the prostate glands of Vav3 transgenic mice. Prostate tissues (magnification, ×400) from Vav3 transgenic mouse (*left*) and wild-type mouse (*right*) were subjected to immunohistochemical analysis for phospho-Akt. *Brown*, immunostaining. *C*, prostate tissue extracts (100 μg) derived from Vav3 transgenic and wild-type mice were subjected to Western blot analysis for Akt and phospho-Akt. β-Actin served as loading control.

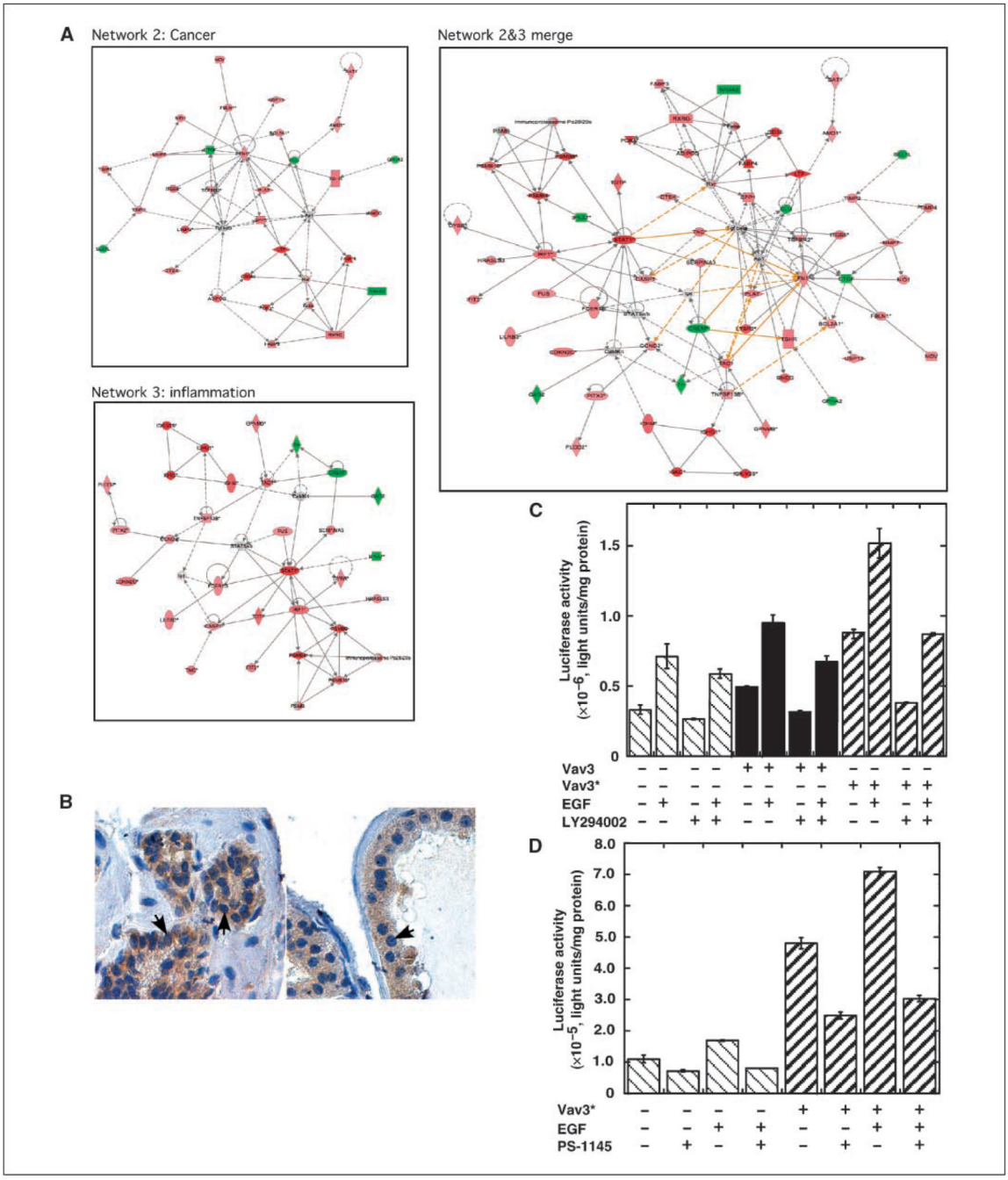

Figure 5.

Alteration of the cancer- and inflammation-related pathways in the prostate glands of Vav3 transgenic mice. *A*, gene expression networks were constructed for genes differentially expressed in the prostate gland between Vav3 transgenic and wild-type mice using the Ingenuity data base. The identified networks on the top of the list are cancer and inflammation, which are merged (*network 2&3 merge*). High magnification of the figures was shown in Supplementary Figs. S1 to S3. *B*, expression analysis of Rel A in the prostate glands of Vav3 transgenic mice. Prostate tissues (magnification, ×600) from Vav3 transgenic mouse (*left*) and wild-type mouse (*right*) were subjected to immunohistochemical analysis for Rel A. *Brown*, immunostaining. *C* and *D*, Vav3 up-regulates NF-κB activity. LNCaP cells (10^5 per well in a

12-well plate) were cotransfected with NF-κB-Luc (0.5 μg) and expression vector for Vav3 or Vav3* (250 ng). Then, the cells were treated without or with EGF (100 ng) and/or LY294002 (10 μmol/L; *C*) or EGF and/or PS-1145 (5 μmol/L; *D*) for 24 h in stripped medium, followed by luciferase assay. Renilla luciferase as an internal control was used to normalize the data. *Columns*, mean of duplicate values of a representative experiment that was independently repeated five times; *bars*, SD.

Table 1

Targeted overexpression of Vav3 in the prostatic epithelium leads to an elevated AR-mediated signaling and prostate cancer

***A*. Histopathologic analysis of the prostate gland from Vav3 transgenic mice**

Age (mo)	Normal	PIN	Cancer	No. mice
Transgenic mice lines 2, 4, and 5				
2–4	0	19	9	28
5–7	0	16	20	36
8–10	0	9	12	21
Total	0	44	41	85
Normal mice				
2–4	5	0	0	5
5–7	3	3	0	6
8–10	0	6	0	6
Total	8	9	0	17

$P < 0.001$ (Fisher's exact test)

***B*. The expression levels of multiple genes in the AR-mediated pathway are elevated in the prostate glands of Vav3 transgenic mice**

Oligo ID	Accession	Gene name	Symbol	TG/WT	*P*
mMR031244	NM_009596	androgen binding protein α	*Abpa*	2.27	0.003217
mMC010072	NM_203502	androgen binding protein β	*Abpb*	3.54	0.003774
mMC025865	NM_194338	androgen binding protein γ	*Abpg*	4.38	0.00075
mMA032501	NM_016900	caveolin 2	*Cav2*	1.35	0.036785
mMC017665	NM_007617	caveolin 3	*Cav3*	1.49	0.05801
mMC023773	NM_007616	caveolin, caveolae protein 1	*Cav1*	1.41	0.031501
mMC024019	NM_010639	kallikrein 1	*Klk1*	2.78	0.000981
mMR030138	NM_011413	sex-limited protein	*Slp*	2.25	0.005395